

# Enhancing COVID-19 Forecasting Precision through the Integration of Compartmental Models, Machine Learning and Variants

Daniele Baccega<sup>1,3,\*</sup>, Paolo Castagno<sup>1</sup>, Antonio Fernández Anta<sup>2</sup>, and Matteo Sereno<sup>1</sup>

<sup>1</sup>Computer Science Department, Università di Torino, Italy

<sup>2</sup>IMDEA Networks Institute, Madrid, Spain

<sup>3</sup>Laboratorio InfoLife, Consorzio Interuniversitario Nazionale per l'Informatica (CINI), Italy

\*[daniele.baccega@unito.it](mailto:daniele.baccega@unito.it)

## ABSTRACT

Predicting epidemic evolution is essential for informed decision-making and guiding the implementation of necessary countermeasures. Computational models are vital tools that provide insights into illness progression and enable early detection, proactive intervention, and targeted preventive measures.

This paper introduces Sybil, a framework that integrates machine learning and variant-aware compartmental models, leveraging a fusion of data-centric and analytic methodologies. To validate and evaluate Sybil's forecasts, we employed COVID-19 data from two European countries. The dataset included the number of new and recovered cases, fatalities, and variant presence over time. We evaluate the forecasting precision of Sybil in periods in which there is a change in the trend of the pandemic evolution or a new variant appears. Results demonstrate that Sybil outperforms a conventional data-centric approach, being able to forecast accurately the changes in the trend, the magnitude of these changes, and the future prevalence of new variants.

Keywords: Artificial Intelligence, Epidemics, Compartment models, Variants, Forecasting, COVID-19

## Introduction

The COVID-19 pandemic, caused by the SARS-CoV-2 virus, highlights the intricate challenges of addressing the most impactful global health crisis of the 21st century. The rapid global spread of the virus has affected nearly every part of the world. Consequently, healthcare systems worldwide are grappling with the significant challenge posed by COVID-19, requiring a continuous COVID-19 monitoring system that includes robust surveillance, widespread testing, contact tracing, and can be used to plan and deploy stringent infection control measures.

Establishing a continuous monitoring system aids policymakers in effectively managing the socio-health emergency brought about by the epidemic. Accurate forecasting is a fundamental element of such a system, and is crucial for efficient planning, resource allocation, and decision-making within public health authorities. It facilitates the development of proactive measures, such as vaccination campaigns, travel advisories, and community engagement programs, fostering public awareness and participation in disease control efforts. This proactive approach enhances preparedness and is critical in curbing the spread of infectious diseases and mitigating their impact on communities worldwide. Epidemic forecasting involves a multidisciplinary approach, integrating epidemiology, mathematical modeling, data analysis, and computational methods to gain insights into the future progression of outbreaks.

Numerous methodologies are available for predicting the future trajectory of an epidemic, leveraging diverse modeling approaches. Particularly, machine learning (ML) models<sup>1-3</sup> and especially deep learning (DL) models, including Convolutional Neural Networks (CNNs), Recurrent Neural Networks (RNNs) featuring Long Short-Term Memory (LSTM) or Gated Recurrent Unit (GRU) cells, and multivariate CNNs<sup>4-6</sup>, have emerged as highly prominent approaches for forecasting. Several studies use a combination of multiple data-centric approaches (e.g., a machine learning model with ARIMA or Prophet<sup>7</sup>). Despite their increasing popularity, surpassing conventional techniques such as auto-regressive models (e.g., ARIMA, SARIMA)<sup>2,5,8</sup>, these data-centric approaches exhibit notable limitations. First of all, predictions are not easily explainable, and secondly, they often fail to predict changes in the trend, such as peaks or the appearance of new variants.

On the other hand, compartmental models<sup>9-11</sup> and stochastic transmission models<sup>12</sup> are analytic approaches specifically tailored to reproduce the evolution of an infection in a population and in the presence of variants<sup>13-16</sup>. These models incorporate factors such as population demographics, rates of infection, recovery, and mortality, providing a mathematical representation of

epidemic progression<sup>17,18</sup>. This transparency simplifies explaining and interpreting the results to policymakers, healthcare professionals, and the general public, thus fostering a better understanding and informed decision-making. Indeed, several COVID-19 forecasting studies incorporate data-centric and analytical approaches, such as a combination of compartmental models and ARIMA<sup>19</sup>, and several other combinations<sup>20</sup>.

Forecasting the epidemic spread aims to accurately predict the percentage of the infected population at a given point in the future, the number of fatalities, hospitalizations, and so on. However, these percentages result from complex population dynamics that often show nonlinear behaviors, particularly at critical points where there are changes in the infection course—such as at the peak of the diffusion or when a new variant arises. Conversely, epidemics dynamics are often characterized by widely recognized quantities. The most well-known is the basic reproduction number,  $R_0$ , which express the number of secondary infection arising from one single infected individual within a population of susceptible individuals. Although  $R_0$  is useful to characterize if and how fast a disease spreads in a population, its time-dependent counterpart,  $R_t$ , enables a quantitative evaluation of the infection course. Such indicators, being specific to the disease, tend to be stable. Therefore, their future evolution shows a more predictable behavior.

Following the approach of combining data-driven approaches with analytical models, we propose **Sybil**, an integrated machine learning and variant-aware compartmental model framework capable of providing improved prediction accuracy and explainability. Sybil exploits the relative stability of disease characteristics indices to project in the future and employs a simple and widely recognized analytical model to draw the infection dynamic. Sybil's strengths mark the difference with approaches present in the literature thanks to *i*) its capability of providing accurate forecasts, even when there are relevant changes in the diffusion process, and *ii*) reduced need for training data. Furthermore, the approach offers *iii*) the possibility to study the evolution of the infection of several variants and *iv*) the replicability of the results. Additionally, *v*) the open-source code is available online.

The joint use of ML and analytical models is gaining momentum in computational epidemiology. Still, to the best of our knowledge, Sybil outperforms the available solutions in several aspects, such as its explainable and reproducible results. For instance, in<sup>19</sup>, the authors use a compartmental model combined with a predictive model of the pandemic to forecast its evolution 60 days in the future, building their approach on the observed data in Kenya. In particular, they propose to estimate the parameters of the compartmental model—precisely the effective reproductive number—using ARIMA and then to use the predicted values to forecast the pandemic with a SEIR compartmental model. Specifically, the authors design a compartmental model accounting for symptomatic and asymptomatic individuals, as well as mild and severe cases. Despite the many similarities, Sybil employs a much simpler compartmental model, which enables us to consider variants and still have a model without significant complexities. Also, using ARIMA makes the approach in<sup>19</sup> less suitable for continuous monitoring platforms. It also makes it harder to apply the same methodology to other scenarios. Eventually, results presented in<sup>19</sup> are not validated against historical data, and the forecasting accuracy is not easy to assess.

## Methods

We propose an integrated framework aimed at providing accurate and explainable predictions for epidemic spreads. Sybil combines a simple compartmental model with a machine learning-based predictive model to forecast the future progression of infection, even in the presence of multiple virus strains. At the core of Sybil, there is a simple analytical model which has a dual functionality. In the first stage of Sybil's operation, the analytical model is used to derive the value of critical model parameters from the surveillance data. Then, these parameters' values—ascrivable to the reproductive number over time,  $R_t$ —are used as training data for the ML component of Sybil. Based on that knowledge, it predicts the future values for the key parameters, which are then plugged back into the analytical model. Then, Sybil computes the future evolution of daily infections using the analytical model with these key parameters' future values.

The performance evaluation of Sybil's forecast is made by *i*) comparing it against the real data coming from the active surveillance of the pandemic situation in several European states and *ii*) comparing it against forecasts obtained by a ML approach. In this latter case, we use Prophet<sup>21</sup> to predict the evolution of the different active variants in the considered period, representing a typical forecasting approach based on ML.

### Compartmental analytical model

The first component of Sybil is the analytical model. In the field of computational epidemiology, compartmental models are widely recognized and employed to study the spreading of an infection in a population. Also, compartmental models are easy to explain: the model contains several compartments, each representing a specific subpopulation, and uses rates to move individuals from one compartment to another. The simplest compartmental model to mimic the evolution of an infection in a population requires only two compartments and one rate; the two compartments represent the only two possible states of the individuals in the population—either susceptible (S) or infected (I)—and one transition rate that represents the pace at which

one infected individual infects a susceptible one. Because of the two states characterizing this model, it is commonly known as the Susceptible-Infected (SI) model.

In order to capture some critical features of the SARS-CoV-2 infection, an SI model is not suitable, and a more complex one is required. Specifically, we need to model the end of the infected period explicitly, i.e., when an infected person recovers from the illness. Additionally, fatalities and reinfections must be taken into account. Hence, the compartmental model incorporated in Sybil has two additional compartments, one accounting for individuals recovered from the infection (R) and one for the deceased (D), with the corresponding rates. Specifically, the model used is a Susceptible-Infected-Recovered-Deceased-Susceptible (SIRDS) compartmental model with reinfections—represented in Figure 1-(a)—that is described by the system of difference equations in Equation 1. In this system,  $\beta$  represents the infection rate,  $\gamma$  the recovery rate,  $\lambda$  the fatality rate,  $\nu$  the end-of-immunization rate, and N the total population.

$$\begin{aligned} S(\tilde{t} + 1) &= S(\tilde{t}) - \beta(\tilde{t}) \frac{S(\tilde{t})I(\tilde{t})}{N} + \nu R(\tilde{t}) \\ I(\tilde{t} + 1) &= I(\tilde{t}) + \beta(\tilde{t}) \frac{S(\tilde{t})I(\tilde{t})}{N} - \gamma(\tilde{t})I(\tilde{t}) - \lambda(\tilde{t})I(\tilde{t}) \\ R(\tilde{t} + 1) &= R(\tilde{t}) + \gamma(\tilde{t})I(\tilde{t}) - \nu R(\tilde{t}) \\ D(\tilde{t} + 1) &= D(\tilde{t}) + \lambda(\tilde{t})I(\tilde{t}) \end{aligned} \quad (1)$$

In this model, the rates are time-dependent—meaning that they may vary at each time step, with the time step corresponding to one day. The only exception is end-of-immunization rate  $\nu$ , which is assumed to be  $\nu = \frac{1}{180}$ , since on average the immunization due to infection is estimated to be lost after 180 days<sup>22</sup>.

Using the surveillance data—possibly after a pre-processing phase—, Sybil computes the evolution of the infection process by solving the SIRDS model in Equation 2, where  $\Delta I(\tilde{t})$  represents the new infected at time  $\tilde{t}$ ,  $\Delta R(\tilde{t})$  the new recoveries at time  $\tilde{t}$  and  $\Delta D(\tilde{t})$  the new deceases at time  $\tilde{t}$  (with  $S(0) = N$  and  $I(0) = R(0) = D(0) = 0$ ).

However, obtaining all the required parameters to solve equations in Equation 1 is not straightforward. Indeed, surveillance data does not provide the transition rates—namely, the bold elements in the system of difference equations—and hence a further step is required: using Equation 3 (obtained from Equation 1), we can estimate the daily infection, recovery, and fatality rates.

$$\begin{aligned} S(\tilde{t} + 1) &= S(\tilde{t}) - \Delta I(\tilde{t}) + \nu R(\tilde{t}) \\ I(\tilde{t} + 1) &= I(\tilde{t}) + \Delta I(\tilde{t}) - \Delta R(\tilde{t}) - \Delta D(\tilde{t}) \\ R(\tilde{t} + 1) &= R(\tilde{t}) + \Delta R(\tilde{t}) - \nu R(\tilde{t}) \\ D(\tilde{t} + 1) &= D(\tilde{t}) + \Delta D(\tilde{t}) \end{aligned} \quad (2)$$

$$\begin{aligned} \lambda(\tilde{t}) &= \frac{D(\tilde{t} + 1) - D(\tilde{t})}{I(\tilde{t})} && \text{if } I(\tilde{t}) > 0 \text{ else } \lambda(\tilde{t}) = 0 \\ \gamma(\tilde{t}) &= \frac{R(\tilde{t} + 1) - R(\tilde{t}) + \nu R(\tilde{t})}{I(\tilde{t})} && \text{if } I(\tilde{t}) > 0 \text{ else } \gamma(\tilde{t}) = 0 \\ \beta(\tilde{t}) &= \frac{I(\tilde{t} + 1) - I(\tilde{t}) + \gamma(\tilde{t})I(\tilde{t}) + \lambda(\tilde{t})I(\tilde{t})}{S(\tilde{t})I(\tilde{t})} N && \text{if } S(\tilde{t})I(\tilde{t}) > 0 \text{ else } \beta(\tilde{t}) = 0 \end{aligned} \quad (3)$$

Bringing in variants into the model of Equation 1 requires introducing one additional compartment to account for infections caused by each virus strain, hence obtaining an SI<sup>V</sup>RDS model, where the superscript at the I stands for the maximum number of virus strains included in the model (see Figure 1-(b)). After introducing further compartments, also additional rates are necessary. Specifically, instead of a global infection rate  $\beta(\tilde{t})$ , there are  $V$  different infection rates—one for each variant—for each time step  $\tilde{t}$ . Making a simplifying assumption, Sybil assumes that the evolution of the  $I_\nu(\tilde{t})$  compartment—for each variant  $\nu$  and for each time step  $\tilde{t}$ —is computed starting from the evolution of the  $I(\tilde{t})$  compartment of the model without variants and the daily proportion of the considered variant; that is,  $I_\nu(\tilde{t}) = I(\tilde{t})\pi_\nu(\tilde{t})$ , where  $\pi_\nu(\tilde{t})$  is the proportion of infections due to variant  $\nu$  at time  $\tilde{t}$ . Moreover, we assumed no correlations among variants and that being recovered from a variant  $\nu$  makes a person immune from all variants (and after  $\frac{1}{\nu}$  days, in average, a person will be susceptible again).

$$I_\nu(\tilde{t} + 1) = I_\nu(\tilde{t}) + \beta_\nu(\tilde{t}) \frac{S(\tilde{t})I(\tilde{t})}{N} - \gamma(\tilde{t})I_\nu(\tilde{t}) - \lambda(\tilde{t})I_\nu(\tilde{t}) \quad \nu \in \{1 \dots V\} \quad (4)$$

$$\beta_v(\tilde{t}) = \frac{I_v(\tilde{t}+1) - I_v(\tilde{t}) + \gamma(\tilde{t})I_v(\tilde{t}) + \lambda(\tilde{t})I_v(\tilde{t})}{S(\tilde{t})I(\tilde{t})} N \quad v \in \{1 \dots V\} \quad (5)$$

1 Equation 4 describes the evolution of the  $I_v$  compartments. Here, we used the previously computed global recovery and  
2 fatality rates, and  $\beta_v(\tilde{t})$  is a column vector with the time-dependent infection rates of  $V$  variants—in the supplementary material  
3 we have detailed these assumptions. Eventually, Equation 5 (obtained from Equation 4) describes how to compute the infection  
4 rates  $\beta_v(\tilde{t})$  for the  $v$  variant.

5 It is worth noticing that in devising infection and fatality rates from surveillance data, we incorporate all the effects due to  
6 the different virus strains and the impact of contention policies, even if such details are not explicitly detailed in the model.

## 7 Prophet predictive model

8 The second component of the Sybil framework is Prophet<sup>21</sup>, an open-source framework developed by Facebook for time series  
9 forecasting. It is based on an additive model design and it has been conceived to have intuitive parameters that can be adjusted  
10 without knowing the details of the underlying model. The modeling approach of Prophet combines the strengths of both  
11 statistical modeling and machine learning techniques; it utilizes a generalized additive model that incorporates piece-wise linear  
12 trends, nonlinear growth, and seasonality adjustments using a Fourier series. This flexible modeling approach enables Prophet  
13 to capture simple and complex data patterns. In particular, it consists of three main model components: trend, seasonality, and  
14 holidays combined in the following equation:

$$y(\tilde{t}) = g(\tilde{t}) + s(\tilde{t}) + h(\tilde{t}) + \varepsilon_{\tilde{t}} \quad (6)$$

15 where  $g(\tilde{t})$  is the trend function that models non-periodic changes,  $s(\tilde{t})$  represents periodic changes (e.g., daily, weekly, and  
16 yearly seasonality), and  $h(\tilde{t})$  represents the effects of holidays which occur on potentially irregular schedules over one or more  
17 days. The error term  $\varepsilon_{\tilde{t}}$  represents any characteristic changes that are not accommodated by the model. Furthermore, Prophet  
18 makes it possible to estimate uncertainty in trend forecasts. It employs Markov Chain Monte Carlo (MCMC) to generate many  
19 plausible future trajectories. The MCMC procedure randomly samples from the posterior distribution of the model parameters,  
20 allowing for a range of possible outcomes. These sampled parameter sets are then used to generate multiple forecast trajectories.

## 21 Data

22 All datasets used in this work are open source and publicly available. The surveillance data used for Italy and Austria in the  
23 *Results* section are available in the COVID19 R library<sup>23,24</sup> (for the results presented in the *Results* section we used a snapshot  
24 dated November 22<sup>nd</sup>, 2023). This data comprises all the data reported in Figures 2 to 6 plus other data not relevant to the  
25 present study—such as the number of vaccinations, tests, hospitalizations and people in intensive care, information about  
26 applied countermeasures, data on mobility, etc. In particular, from the COVID-19 Data Hub<sup>23,24</sup>, we used the following data  
27 (from February 2020 to May 2023): the cumulative number of cases, the cumulative number of recoveries, the cumulative  
28 number of deaths, and the total population. Starting from these, we computed the daily new cases, the daily new recoveries, and  
29 the daily new deaths we used in Equation 2.

30 Information about active virus strains comes from the European Center for Disease Control (ECDC), specifically, the  
31 one reported in<sup>25,26</sup> (for the results presented in the *Results* section we used a snapshot dated July 25<sup>th</sup>, 2023). Here, ECDC  
32 collected the result of serological tests, and there is information about a significant number of variant lineages, such as B.1.1.7,  
33 BA.1, BA.2, P.1, XBB, and many others. To use such data, we aggregated these lineages in four main variant families with the  
34 aim of using the WHO variants labels: Alpha, Delta, Omicron, and *Other*<sup>27</sup>. In particular, the *Other* variant comprises the  
35 initial SARS-CoV-2 lineage, all the other lineages (e.g., Beta, Gamma, Kappa), and some noisy values in the surveillance data.

36 Since variants' diffusion data is provided weekly, in a pre-processing phase, we expanded such data to devise approximated  
37 daily values. Specifically, we employed splines—piece-wise-defined mathematical functions that use multiple polynomial  
38 segments to create a smooth and continuous curve—to obtain daily values.

39 In the following section, we used time-dependent recovery rates thanks to data availability for the selected countries—  
40 namely Italy and Austria. However, surveillance data available for many countries worldwide does not report data to devise  
41 daily recovery rates. Hence, to dispense with data on recoveries, in the supplementary material we report results obtained with  
42 fixed recovery rate with mean  $\frac{1}{\gamma}$  equals to 14 days—same for each variant. The results obtained are promising and show the  
43 robustness of the Sybil approach.

## 44 Results

45 This section starts focusing on surveillance data from Italy and spanning a period from February 2020 to May 2023. During  
46 this period, there are a significant number of lineages, some coexisting and others with an evolutionary advantage taking over.  
47 In Figure 2, lineages are aggregated into the four main variants introduced above.



1 Accurate forecasts strongly depend on the regularity of the data to predict: it is pretty easy to foresee the future evolution of  
2 some dimensions increasing—or equally decreasing—linearly. Conversely, predicting the behavior in the presence of sudden  
3 changes in those quantities is much harder. Unfortunately, outbreaks, as well as peak infection fading, exhibit such a behavior.  
4 Vertical dashed lines in Figure 2 mark the time point picked to evaluate the accuracy of Sybil. The first two selected points  
5 are placed in the ascending part of an outbreak but close enough to the peak for accurate predictions, Sybil must successfully  
6 reproduce a change in the concavity of the function. The third selected point is placed just before the start of Omicron’s  
7 outbreak to show that Sybil is also able to predict a new emerging variant/outbreak. Further experiments and scenarios are  
8 available in the supplementary material.

9 The first forecast scenario corresponds to the first infection wave, which in Italy started in February 2020. Only one  
10 SARS-CoV-2 strain was detected during this initial wave, namely the *Other* variant of Figure 2. Figure 3-(a) reports four  
11 different forecasts, all starting on April 15<sup>th</sup> 2020 and spanning several forecast windows—from one to four weeks. For each  
12 forecasting window, we compare predictions obtained using Sybil (green line) and the standard approach used in the literature  
13 (red line), which requires using the selected forecasting approach—Prophet in our case—to project the number of infections  
14 in the coming weeks. The two approaches use the same period as training data (black line) for a fair comparison. They are  
15 compared and contrasted against the surveillance data for the period spanning the forecasting window (blue line). Comparing  
16 predictions obtained with the plain use of Prophet to forecast the evolution of the number of daily infections, we notice that it  
17 fails to predict the plateau characterizing the highest part of the peak. Considering Sybil’s predictions, we see that starting from  
18 short-term predictions—i.e., seven days—it catches the decreasing trend. Increasing the forecasting window, Sybil always  
19 provides an excellent approximation of the future evolution of the daily infections, but for four weeks. In this latter case,  
20 Sybil’s predictions diverge in magnitude from the ground truth, but not in trend. It provides a qualitative indication of the future  
21 evolution of the pandemic, which eventually fades. Figure 3-(b) shows the infection rate  $\beta_v(\bar{t})$  for the observation period. Here,  
22 we clearly see that the values for the infection rate are noisy; what we see is not a smooth line, but saw-tooth function with  
23 many peaks and valleys. Nonetheless, the range of variation of that function is limited and with a clear trend, which Sybil easily  
24 learns and replicates.

25 The second scenario considers a period spanning the highest peak in the data set. Here, we consider the period from  
26 December 13<sup>th</sup> 2021 to January 13<sup>th</sup> 2022 as training data, and we forecast the daily infections for the period January-February  
27 2022 (starting from January 14<sup>th</sup>). In Italy, there were three active variants within this time window: Omicron, Delta, and the  
28 *Other* variant. Figure 4-(a) shows the number of daily infections for the three active variants and compares the ground truth  
29 (dashed line) with Sybil’s forecasts for one to four weeks. Again, forecasts are highly accurate for seven to twenty-one days  
30 long predictions and slightly anticipate the peak’s descendent phase at four weeks. In Figure 4-(b), the two approaches are  
31 contrasted against the ground truth. Like the first scenario, the Prophet’s predictions do not capture the peak. Not only do  
32 Prophet’s predictions get far from the real data—they grow while the infection fades—but, in this scenario, they do not even  
33 provide a valid qualitative prediction.

34 The third point picked to test Sybil’s predictions falls just before the explosion of the largest outbreak caused by the Omicron  
35 variant. In particular, Figure 5 shows how the one-week forecast changes moving the training window from December 18<sup>th</sup>,  
36 2021 to December 27<sup>th</sup>, 2021. In this scenario, the ascending trajectory is very steep, and Sybil finds it harder to calibrate with  
37 respect to the previous cases. Here, the Omicron variant is a new emerging variant and Sybil initially foresees a more aggressive  
38 exponential growth. Looking at Figure 5 we can state that Sybil nailed the qualitative prediction, but needed more data to  
39 calibrate it. We can also see that Sybil captures well the prediction on the other active variant—the Delta variant. Here we are  
40 showing the best results obtained in this scenario. In the supplementary material we provide more details on this scenario and  
41 show another case where an explosive outbreak occurs, discussing the convenience of establishing a continuous monitoring  
42 system.

43 Sybil provides a robust, easily portable approach to different use cases without requiring modifications. For instance, in  
44 Figure 6 we apply Sybil to surveillance data from Austria. Figure 6-(a) shows the daily infections for the different SARS-CoV-2  
45 strains active in the period from February 2020 to May 2023. As in the case of Italy, lineages are grouped into four main virus  
46 strains—Alpha, Delta, Omicron, and the *Other* variant. In Figure 6-(b), data from January 1<sup>st</sup> 2022 to February 1<sup>st</sup> 2022 are  
47 employed to train the models, and we compare forecasts obtained for February 2022 (starting from February 2<sup>nd</sup>). During this  
48 period, there were two active variants: Omicron and the *Other* variant, as in the second scenario considered for Italy. The initial  
49 point chosen for the forecasts is again placed in the surroundings of the highest peak so that correctly predicting the future  
50 evolution of the infection is much more challenging. Nonetheless, Sybil shows high accuracy in predicting the future trajectory  
51 of the infection; despite a slightly different evolution, Sybil correctly predicts the diffusion slowdown, the successive decreasing  
52 phase. Eventually, prediction and surveillance data meet at the end of the four-week-long forecast.

## 1 Discussion

2 ML approaches have already shown their power when dealing with complexity, thanks to their excellent capabilities in exploiting  
3 non-trivial correlations often inaccessible with other tools. Despite the many advantages of employing ML approaches, there  
4 are also some caveats worth noting. First, most of these approaches require a tremendous amount of data to learn from, and  
5 data available from the surveillance might not be enough for most ML approaches. Sybil faces this issue from two different  
6 standpoints; it employs Prophet, a hybrid approach, using ML techniques in combination with simulations—refer to the  
7 *Prophet predictive model* subsection for further details. On the other hand, Sybil does not face the challenge of forecasting the  
8 virus spread as a single task. First, it tries to predict the rates and then computes the future dynamics using a compartmental  
9 model. Therefore, Sybil, combining Prophet and compartmental models, exploits the two approaches in the respective field  
10 of application—where they perform the best—and strengthens the individual weaknesses. Specifically, by providing the  
11 compartmental model with parameters extracted from the real data or forecasts, there is no need to tune the model and estimate  
12 the missing parameters. Estimating model's parameters is a resource-demanding and time-consuming task. Also, it is an  
13 activity tightly related to the specific situation or scenario under evaluation. This makes the model almost impossible to apply  
14 in a different setting without estimating the parameters again. Hence, Prophet makes Sybil's approach easily deployable in  
15 new scenarios without requiring additional tasks, but the data must comply with the daily requirement. Likewise, the use of  
16 compartmental models in predicting the future trend of the infection makes results more straightforward to explain, for instance,  
17 to policymakers, who often do not trust predictions without a robust interpretation.

18 In the *Results* section, we presented Sybil's forecasts of different lengths for several European states and periods spanning  
19 from February 2020 to May 2023. To showcase Sybil's capabilities, all the forecasting periods cover important changes in  
20 the first derivative of the number of daily infections. Then, Sybil's predictions are contrasted against the surveillance data  
21 and the plain application of Prophet. Results shows the superiority of Sybil's approach on the plain forecast of the number of  
22 daily infections; in particular, Sybil outperforms the plain application of Prophet when primary changes in the virus diffusion  
23 happens. For instance, Figure 4-(b) clearly shows the added value of Sybil approach: it predicts with great accuracy the peak  
24 of the current wave while Prophet alone fails to predict the decreasing phase of the infection peak. Further experiments and  
25 scenarios are available in the supplementary material. Here, for instance, some experiments made choosing forecasting periods  
26 far from peaks show that similar and accurate forecasting can be obtained using both approaches and new variants rising or new  
27 outbreaks can be predicted accurately using Sybil to set up a continuous monitoring system.

28 The presented methodology is very close to being a continuous monitoring system, but strongly depends on the availability  
29 of data. In particular, in<sup>23,24</sup> there are few nations with a complete time series (with a daily step) for the data we used (i.e.,  
30 cumulative number of cases, cumulative number of deceases, cumulative number of recoveries). Possible extensions to this  
31 methodology would be to use a fixed recovery rate—same or different for each variant—to dispense with data on recoveries  
32 which are often not available—in the supplementary material we show some results related to this extension—and to include a  
33 pre-processing step using a technique (e.g., splines) to fill missing data and to move from a weekly to a daily step in case of  
34 availability of data with a weekly step—without alter too much the information present in the time series.

## 35 Conclusion

36 The global COVID-19 pandemic has brought to light the urgent necessity for sophisticated tools capable of monitoring and  
37 predicting the trajectory of infections within the population. This paper introduces a cutting-edge framework designed for  
38 continuous monitoring and forecasting, seamlessly integrating machine learning-based predictive models with compartmental  
39 models.

40 Sybil distinguishes itself by delivering forecasts that are not only reliable but also readily explainable, as evidenced by  
41 thorough experimental validation. The adaptability of this innovative approach is clearly demonstrated through its successful  
42 application to diverse surveillance data from two European countries, specifically Italy and Austria.

43 By integrating data-centric and analytic approaches, Sybil effectively addresses the inherent limitations of each method.  
44 This amalgamation not only enhances the tool's ability to forecast the evolution of COVID-19 but also positions Sybil as a  
45 versatile instrument for predicting the trajectory of various other diseases, thus broadening its scope and impact in the field of  
46 infectious disease modeling.

## 47 References

- 48 1. Battineni, G., Chintalapudi, N. & Amenta, F. Forecasting of covid-19 epidemic size in four high hitting nations (usa, brazil,  
49 india and russia) by fb-prophet machine learning model. *Appl. Comput. Informatics* DOI: [10.1108/ACI-09-2020-0059](https://doi.org/10.1108/ACI-09-2020-0059)  
50 (2020).
- 51 2. Zhao, D., Zhang, R., Zhang, H. & He, S. Prediction of global omicron pandemic using arima, mlr, and prophet models. *Sci.*  
52 *reports* **12**, 18138, DOI: <https://doi.org/10.1038/s41598-022-23154-4> (2022).

- 1 **3.** Wang, P., Zheng, X., Li, J. & Zhu, B. Prediction of epidemic trends in covid-19 with logistic model and machine learning  
2 technics. *Chaos, Solitons & Fractals* **139**, 110058, DOI: <https://doi.org/10.1016/j.chaos.2020.110058> (2020).
- 3 **4.** Nabi, K. N., Tahmid, M. T., Rafi, A., Kader, M. E. & Haider, M. A. Forecasting covid-19 cases: A comparative analysis  
4 between recurrent and convolutional neural networks. *Results Phys.* **24**, 104137, DOI: [https://doi.org/10.1016/j.rinp.2021.](https://doi.org/10.1016/j.rinp.2021.104137)  
5 [104137](https://doi.org/10.1016/j.rinp.2021.104137) (2021).
- 6 **5.** ArunKumar, K., Kalaga, D. V., Mohan Sai Kumar, C., Kawaji, M. & Brenza, T. M. Comparative analysis of gated  
7 recurrent units (gru), long short-term memory (lstm) cells, autoregressive integrated moving average (arima), seasonal  
8 autoregressive integrated moving average (sarima) for forecasting covid-19 trends. *Alex. Eng. J.* **61**, 7585–7603, DOI:  
9 <https://doi.org/10.1016/j.aej.2022.01.011> (2022).
- 10 **6.** Kamalov, F., Rajab, K., Cherukuri, A. K., Elnagar, A. & Safaraliev, M. Deep learning for covid-19 forecasting: State-of-  
11 the-art review. *Neurocomputing* **511**, 142–154, DOI: <https://doi.org/10.1016/j.neucom.2022.09.005> (2022).
- 12 **7.** Sardar, I., Akbar, M. A., Leiva, V., Alsanad, A. & Mishra, P. Machine learning and automatic arima/prophet models-based  
13 forecasting of covid-19: Methodology, evaluation, and case study in saarc countries. *Stoch. Environ. Res. Risk Assess.* **37**,  
14 345–359, DOI: [10.1007/s00477-022-02307-x](https://doi.org/10.1007/s00477-022-02307-x) (2023).
- 15 **8.** Alabdulrazzaq, H. *et al.* On the accuracy of arima based prediction of covid-19 spread. *Results Phys.* **27**, 104509, DOI:  
16 <https://doi.org/10.1016/j.rinp.2021.104509> (2021).
- 17 **9.** Fošnarčič, M., Kamenšek, T., Žganec Gros, J. & Žibert, J. Extended compartmental model for modeling covid-19 epidemic  
18 in slovenia. *Sci. reports* **12**, 16916, DOI: <https://doi.org/10.1038/s41598-022-21612-7> (2022).
- 19 **10.** Zhang, P. *et al.* Usage of compartmental models in predicting covid-19 outbreaks. *The AAPS J.* **24**, 98 (2022).
- 20 **11.** He, S., Tang, S., Rong, L. *et al.* A discrete stochastic model of the covid-19 outbreak: Forecast and control. *Math. Biosci.*  
21 *Eng* **17**, 2792–2804 (2020).
- 22 **12.** Kucharski, A. J. *et al.* Early dynamics of transmission and control of covid-19: a mathematical modelling study. *The lancet*  
23 *infectious diseases* **20**, 553–558, DOI: [https://doi.org/10.1016/S1473-3099\(20\)30144-4](https://doi.org/10.1016/S1473-3099(20)30144-4) (2020).
- 24 **13.** Caldwell, J. M. *et al.* Vaccines and variants: Modelling insights into emerging issues in covid-19 epidemiology. *Paediatr.*  
25 *Respir. Rev.* **39**, 32–39, DOI: [10.1016/j.prrv.2021.07.002](https://doi.org/10.1016/j.prrv.2021.07.002) (2021).
- 26 **14.** Rendana, M. & Idris, W. M. R. New covid-19 variant (b. 1.1. 7): forecasting the occasion of virus and the related  
27 meteorological factors. *J. infection public health* **14**, 1320–1327, DOI: [10.1016/j.jiph.2021.05.019](https://doi.org/10.1016/j.jiph.2021.05.019) (2021).
- 28 **15.** Rashed, E. A., Kodera, S. & Hirata, A. Covid-19 forecasting using new viral variants and vaccination effectiveness models.  
29 *Comput. Biol. Medicine* **149**, 105986, DOI: <https://doi.org/10.1016/j.combiomed.2022.105986> (2022).
- 30 **16.** Miller, J. K., Elenberg, K. & Dubrawski, A. Forecasting emergence of covid-19 variants of concern. *Plos one* **17**, e0264198,  
31 DOI: <https://doi.org/10.1371/journal.pone.0264198> (2022).
- 32 **17.** Brauer, F. Compartmental models in epidemiology. *Math. epidemiology* 19–79, DOI: [10.1007/978-3-540-78911-6\\_2](https://doi.org/10.1007/978-3-540-78911-6_2)  
33 (2008).
- 34 **18.** Tolles, J. & Luong, T. Modeling epidemics with compartmental models. *Jama* **323**, 2515–2516, DOI: [10.1001/jama.2020.](https://doi.org/10.1001/jama.2020.8420)  
35 [8420](https://doi.org/10.1001/jama.2020.8420) (2020).
- 36 **19.** Kiarie, J., Mwalili, S. & Mbogo, R. Forecasting the spread of the covid-19 pandemic in kenya using seir and arima models.  
37 *Infect. Dis. Model.* **7**, 179–188, DOI: [10.1016/j.idm.2022.05.001](https://doi.org/10.1016/j.idm.2022.05.001) (2022).
- 38 **20.** Rahimi, I., Chen, F. & Gandomi, A. H. A review on covid-19 forecasting models. *Neural Comput. Appl.* 1–11, DOI:  
39 <https://doi.org/10.1007/s00521-020-05626-8> (2021).
- 40 **21.** Taylor, S. J. & Letham, B. Forecasting at scale. *The Am. Stat.* **72**, 37–45, DOI: [0.7287/peerj.preprints.3190v2](https://doi.org/10.7287/peerj.preprints.3190v2) (2018).
- 41 **22.** West, J., Everden, S. & Nikitas, N. A case of covid-19 reinfection in the uk. *Clin. medicine* **21**, e52, DOI: [10.7861/clinmed.](https://doi.org/10.7861/clinmed.2020-0912)  
42 [2020-0912](https://doi.org/10.7861/clinmed.2020-0912) (2021).
- 43 **23.** Guidotti, E. & Ardia, D. Covid-19 data hub. *J. Open Source Softw.* **5**, 2376, DOI: [10.21105/joss.02376](https://doi.org/10.21105/joss.02376) (2020).
- 44 **24.** Guidotti, E. A worldwide epidemiological database for covid-19 at fine-grained spatial resolution. *Sci. Data* **9**, 112, DOI:  
45 [10.1038/s41597-022-01245-1](https://doi.org/10.1038/s41597-022-01245-1) (2022).
- 46 **25.** for Disease Prevention, E. C. & (ECDC), C. Data on SARS-CoV-2 variants in the EU/EEA.
- 47 **26.** Khare, S. *et al.* Gisaid’s role in pandemic response. *China CDC weekly* **3**, 1049, DOI: [10.46234/ccdcw2021.255](https://doi.org/10.46234/ccdcw2021.255) (2021).
- 48 **27.** Hodcroft, E. B. Covariants: Sars-cov-2 mutations and variants of interest. (2021).

## 1 **Acknowledgements**

2 D.B. is a Ph.D. student enrolled in the National Ph.D. in Artificial Intelligence, XXXVII cycle, health and life sciences course  
3 organized by Università Campus Bio-Medico di Roma.

## 4 **Author contributions statement**

5 D.B. discussed, developed and tested the framework, conceived and conducted the experiments. P.C., A.F.A. and M.S. discussed  
6 and designed the framework, conceived the experiments. All authors reviewed the manuscript.

## 7 **Additional information**

### 8 **Availability of materials and data**

9 COVID-19 data used in this study are available in the COVID19 R library<sup>23,24</sup> and in the ECDC variants data<sup>25,26</sup>. The  
10 framework developed for the analysis presented in this work is available at <https://github.com/daniele-baccega/sybil-forecasting>. To reproduce the results, see supplementary material.

### 12 **Competing interests**

13 All authors declare no competing interests.

### 14 **Funding**

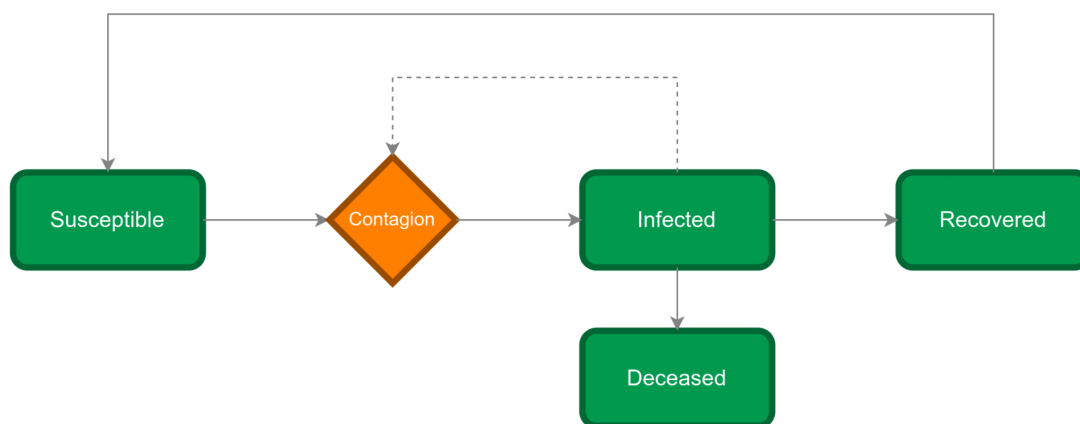
15 This work was supported by grants from “Ripresa delle attività socio-economiche e delle scuole: modelli per la progettazione e  
16 supporto di linee guida per la convivenza con il Covid-19” (Cod. ROL 73459, 2020, PI Matteo Sereno), project funded by CRT  
17 foundation.

### 18 **Supplementary information**

19 A pdf file providing more information on the proposed framework with more scenarios and an extended analysis.

## Figures

a)



b)

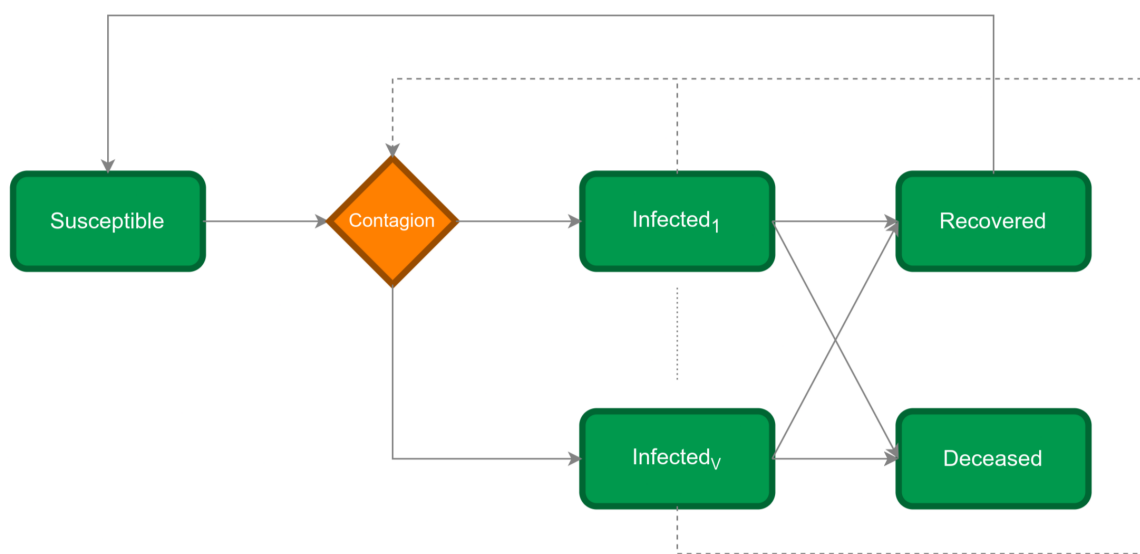


**Figure 1.** Compartmental models: (a) SIRDS and (b)  $SI^V$ RDS. Dashed lines refer to the fact that an infection is due to contacts among susceptible and infected individuals.



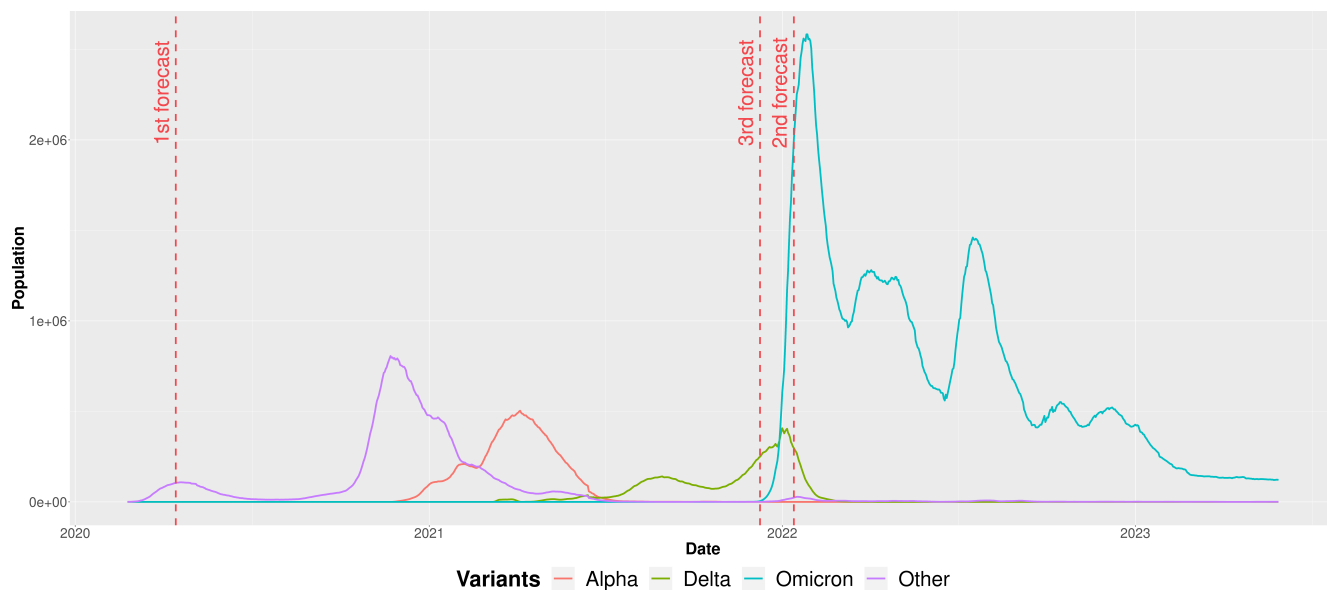


**Figure 2.** Daily active cases in Italy from February 2020 to May 2023 for the four main SARS-CoV-2 strains. Vertical dashed lines mark the selected dates to test Sybil's forecasting.

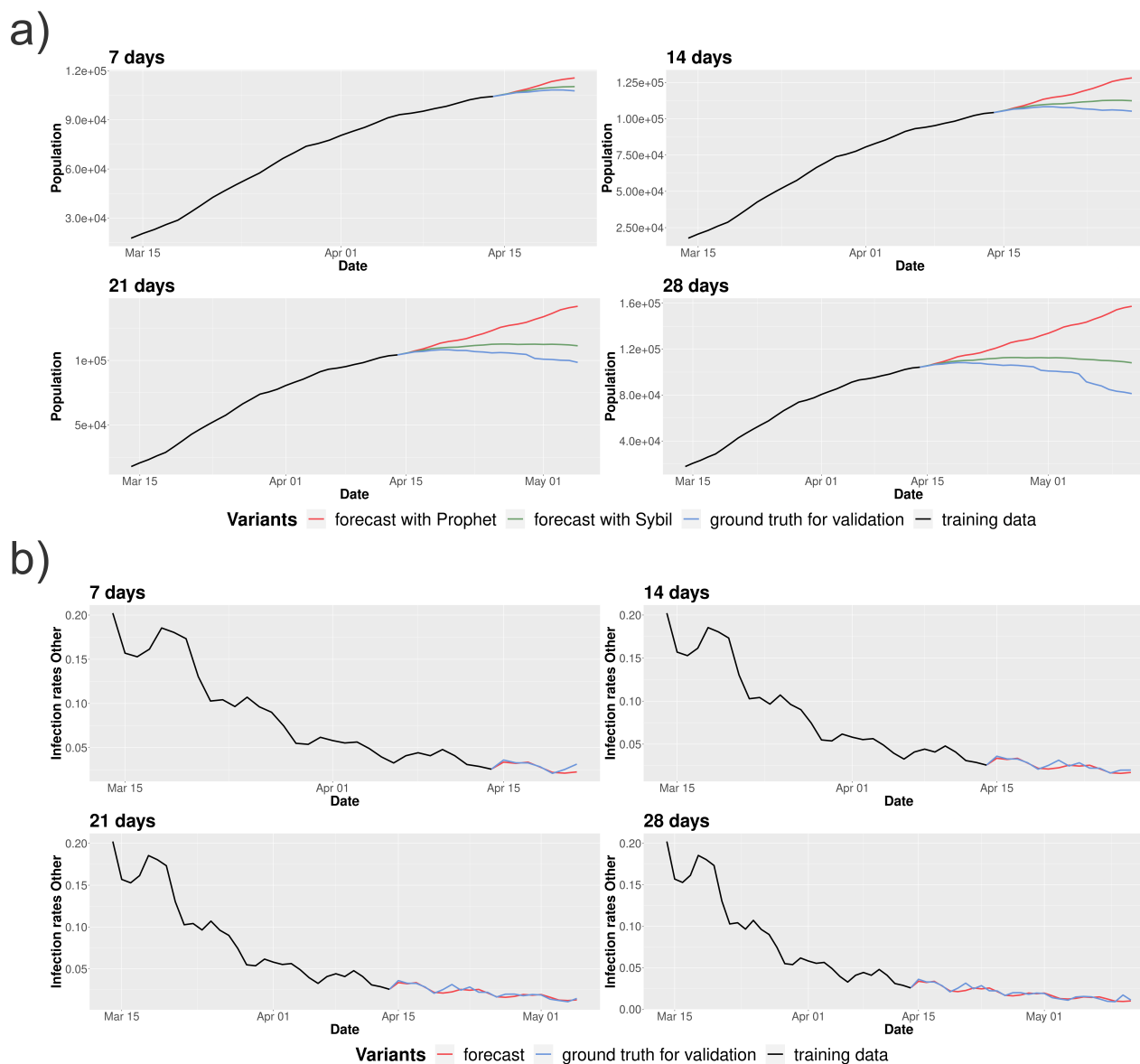


**Figure 3.** The figures refer to the first scenario in which we forecast starting from April 14<sup>th</sup> 2020. Figure (a) shows the evolution of infections using Sybil (green line) and Prophet (red line) using the same period as training data (black line) comparing and contrasting the predictions against the surveillance data for the period spanning the forecasting window (blue line). Figure (b) shows Sybil applied on the infection rate  $\beta_v(\tilde{t})$  of the *Other* variant (the red line shows the prediction, while black and blue lines represent the training data and the ground-truth values extracted from the surveillance data, respectively).

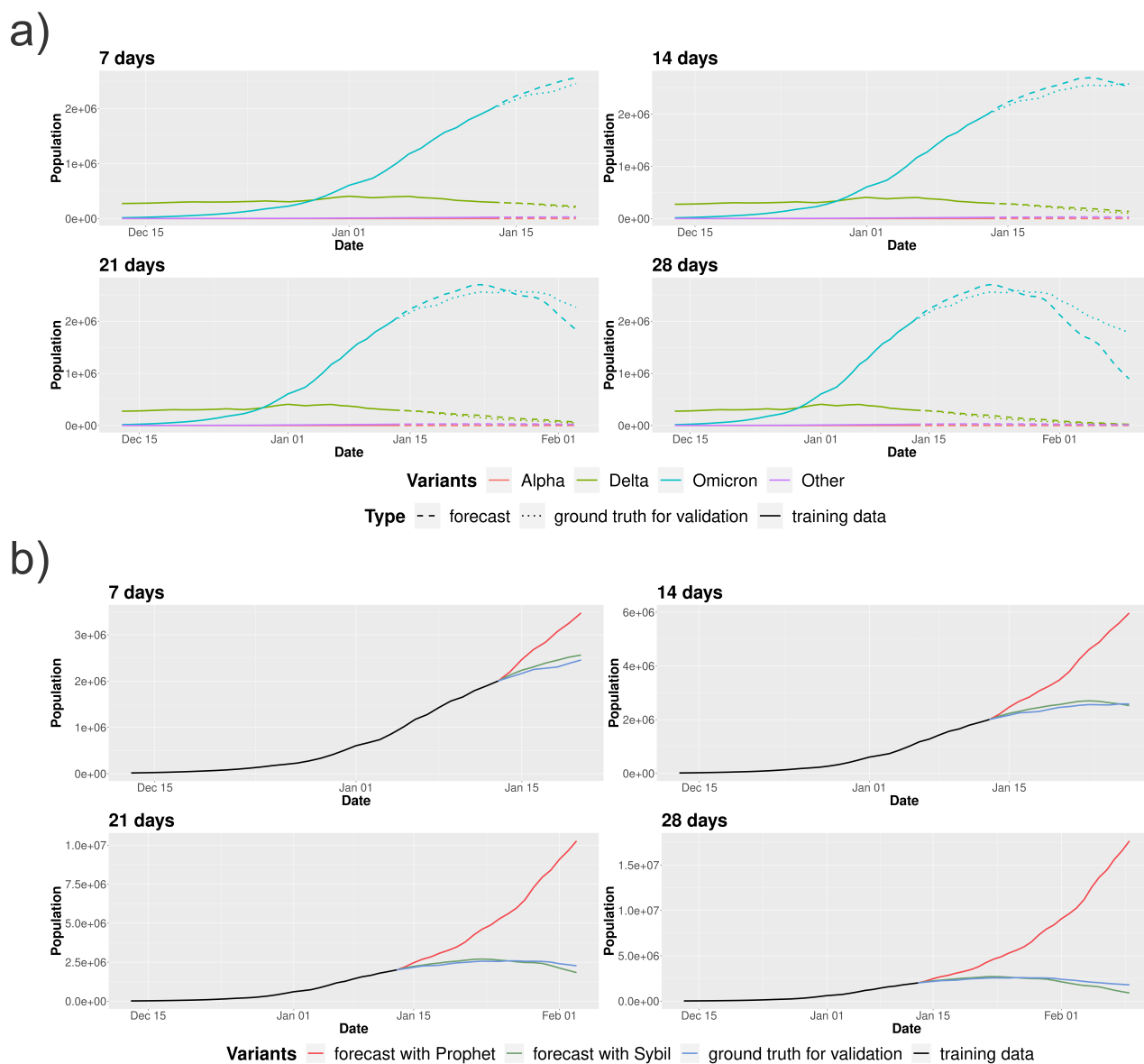


**Figure 4.** The figures refer to the second scenario in which we forecast starting from January 13<sup>th</sup> 2022. Figure (a) show the evolution of infections using Sybil (the dashed line shows the prediction, while solid and dotted lines represent the training data and the ground-truth values extracted from the surveillance data, respectively). Figure (b) shows the comparison between Sybil (green line) and Prophet (red line) on the number of infections for the Omicron variant using the same period as training data (black line) comparing and contrasting the predictions against the surveillance data for the period spanning the forecasting window (blue line).

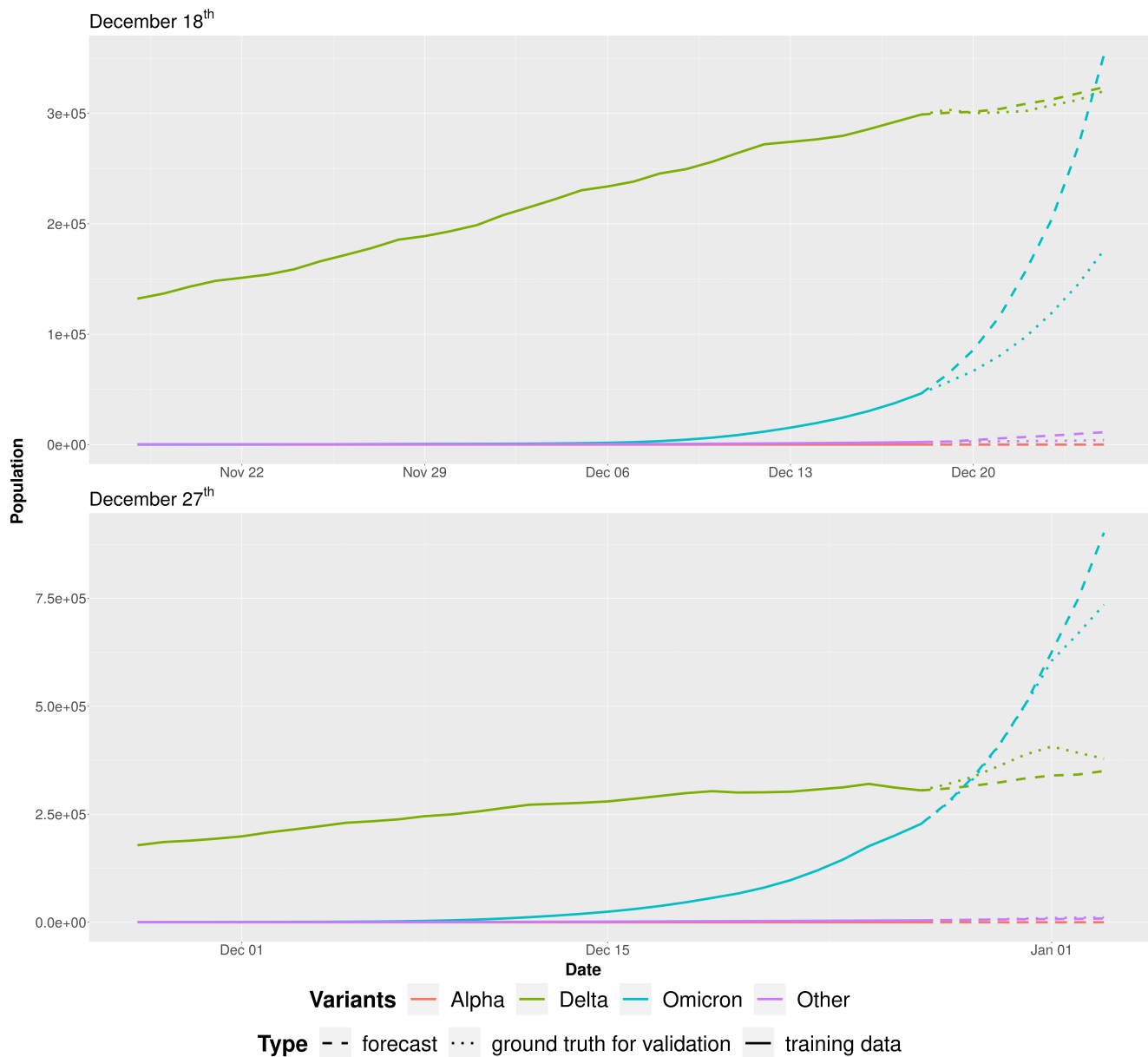


**Figure 5.** Evolution of infections using Sybil on the third scenario. In the first plot we forecast starting from December 18<sup>th</sup>, 2021, while in second one we forecast starting from December 27<sup>th</sup>, 2021. Both the plots refer to a forecast one week into the future. The dashed line shows the prediction, while solid and dotted lines represent the training data and the ground-truth values extracted from the surveillance data, respectively.

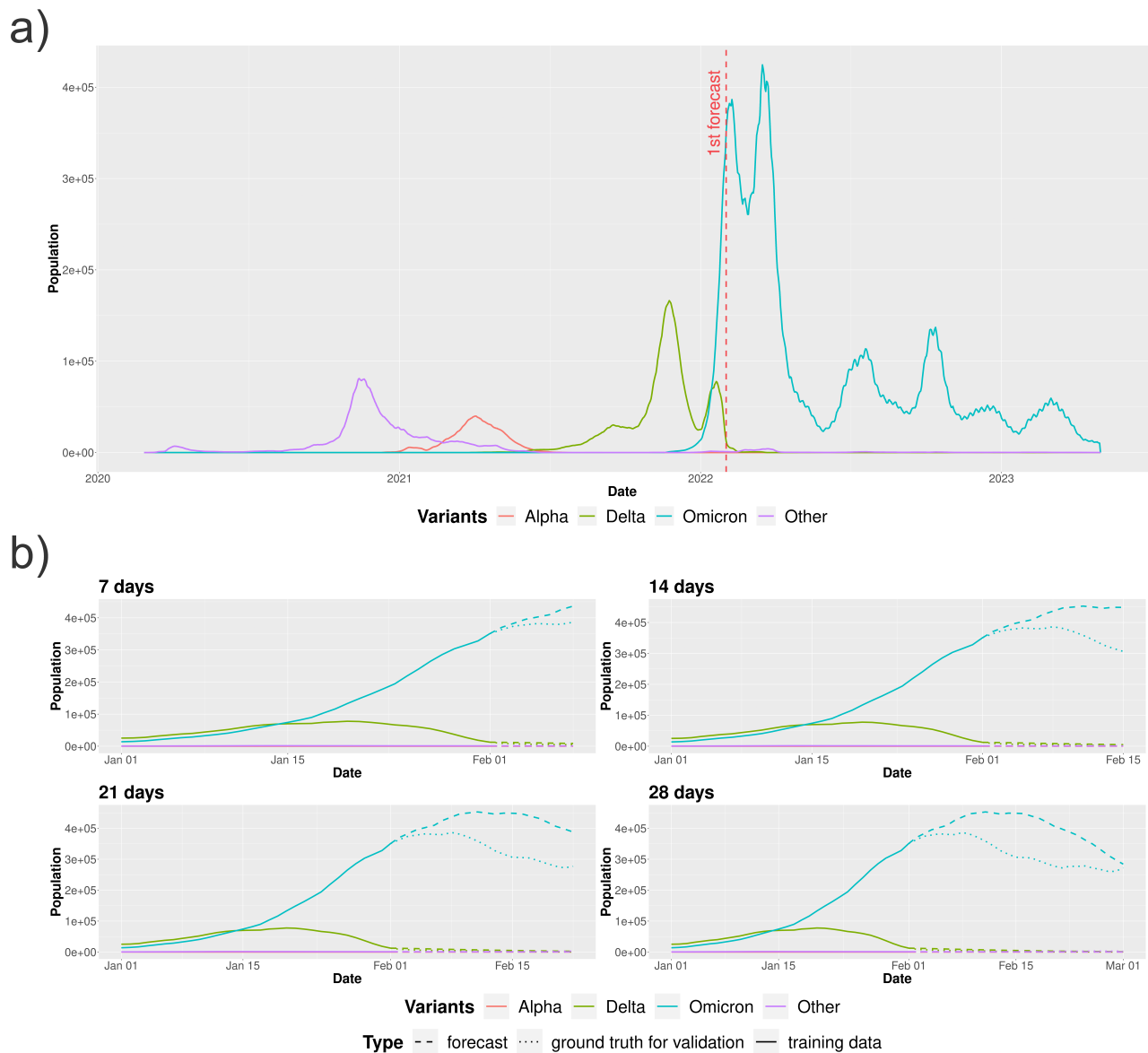


**Figure 6.** The figures show (a) the evolution of infections from February 2020 to May 2023 in Austria with the considered forecast scenario and (b) the evolution of infections using Sybil on the considered scenario in which we forecast starting from February 1<sup>st</sup> 2022 (the dashed line shows the prediction, while solid and dotted lines represent the training data and the ground-truth values extracted from the surveillance data, respectively).